Journal of Power Sources 390 (2018) 78–86

Contents lists available at ScienceDirect

Journal of Power Sources

journal homepage: www.elsevier.com/locate/jpowsour

The reactivity of charged positive $Li_{1-n}[Ni_xMn_yCo_z]O_2$ electrodes with electrolyte at elevated temperatures using accelerating rate calorimetry

Que Huang[a], Lin Ma[b], Aaron Liu[b], Xiaowei Ma[c], Jing Li[c], Jian Wang[a,*], J.R. Dahn[b,c,**]

[a] State Key Laboratory of Fire Science, University of Science and Technology of China, Hefei, China
[b] Department of Chemistry, Dalhousie University, Halifax B3H 4R2, Canada
[c] Department of Physics and Atmospheric Science, Dalhousie University, Halifax B3H 4R2, Canada

HIGHLIGHTS

- Accelerating rate calorimetry is used to explore NMC/electrode reactivity.
- Single crystal NMC532 is less reactive than standard polycrystalline NMC532.
- Various coatings on NMC622 did little to limit reactivity.
- Reactivity increases strongly as the voltage increases.

ARTICLE INFO

Keywords:
Accelerating rate calorimetry
Lithium ion batteries
Safety
Positive electrode reactivity
Elevated temperature
Electrolytes

ABSTRACT

The reactivity between charged positive electrodes of (NMC) and traditional carbonate-based electrolyte (1.09 mol/kg $LiPF_6$ in ethylene carbonate (EC):ethyl methyl carbonate (EMC) (3:7 by weight)) with or without different electrolyte additives at elevated temperatures was methodically investigated using accelerating rate calorimetry (ARC). NMC samples studied included single crystal $Li_{1-n}[Ni_{0.5}Mn_{0.3}Co_{0.2}]O_2$ (SC-NMC532), Al_2O_3-coated $Li_{1-n}[Ni_{0.6}Mn_{0.2}Co_{0.2}]O_2$ (NMC622A) and $Li_{1-n}[Ni_{0.6}Mn_{0.2}Co_{0.2}]O_2$ coated with a proprietary high voltage coating material (NMC622B). The results from this work are compared to previous studies of other NMC materials made using the same methods to build a "library" of comparative results. The ARC results illustrate that the upper cut-off potential and sample morphology, influence the thermal stability of NMC materials, while additives and coatings have a smaller effect. Some outcomes of the work are that the single crystal morphology of NMC532 appears to lead to enhanced thermal stability compared to traditional NMC532 morphology and that NMC811 is significantly more reactive than all the other grades.

1. Introduction

$Li_{1-n}[Ni_xMn_yCo_z]O_2$ (NMC) positive electrode materials for lithium-ion batteries have high specific capacity, relatively low cost and can be used to make large format Li-ion cells with good safety characteristics [1]. Various NMC grades were compared by Kim et al. [2] in a wonderful review article where it was shown that specific capacity (to a fixed upper cutoff potential of 4.3 V increased with the Ni content while the thermal stability of the charged materials in electrolyte and the cycle life decreased with Ni content). Therefore, various tradeoffs must be made when selecting an appropriate positive electrode for a particular application.

Ma et al. [3] compared the reactivity of several kinds of NMC grades charged to different cut-off voltages with traditional carbonate-based electrolyte at elevated temperatures using accelerating rate calorimetry (ARC). According to that article, increasing Ni content and decreasing Mn and Co contents would generally decrease the thermal stability of charged NMC grades in electrolyte. The materials studied by Ma et al. [3] were "standard" NMC materials made from hydroxide precursors having traditional NMC morphology consisting of spherical secondary particles about 10 micrometers in diameter made up of secondary particles about 250 nm in diameter. The materials studied were not coated with thin layers of oxides or other materials to improve lifetime.

Since the time of the Ma et al. [3] work, single crystal NMC grades have become available [4] and it is very important to determine and verify if the single crystal morphology leads to thermal stability advantages over the traditional polycrystalline morphology [5]. Such experiments on single crystal NMC532 (called SC-NMC532 here) were

* Corresponding author.
** Corresponding author. Department of Chemistry, Dalhousie University, Halifax B3H 4R2, Canada.
E-mail addresses: wangj@ustc.edu.cn (J. Wang), jeff.dahn@dal.ca (J.R. Dahn).

https://doi.org/10.1016/j.jpowsour.2018.04.036
Received 1 February 2018; Received in revised form 25 March 2018; Accepted 9 April 2018
Available online 24 April 2018
0378-7753/

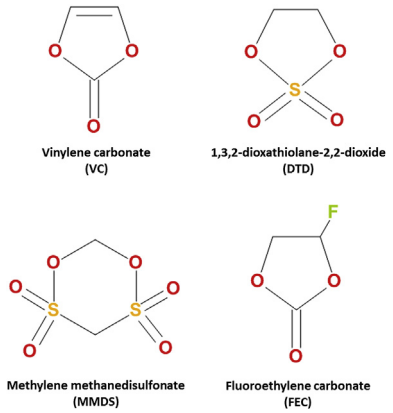

Fig. 1. Chemical structures of the electrolyte additives used in this work.

carried out here. In addition, coatings, like Al_2O_3 on NMC grades have also become more popular and it is important to determine how coatings impact thermal stability of charged electrode materials. Such experiments on Al_2O_3-coated NMC622 (called NMC622A here) and a proprietary coated NMC622 (called NMC622B here) are also carried out here.

In order to reduce the rates of parasitic reactions between charged electrodes and electrolyte, electrolyte additives are often utilized [6,7]. Vinylene carbonate (VC) is one of the most commonly used additives to optimize LIB performance [8,9]. Besides VC, ethylene sulfate (DTD) and methylene methanedisulfonate (MMDS) have also been studied for SC-NMC532 and NMC622 materials, respectively [10]. These electrolyte additives are able to extend lifetime and limit impedance increase for lithium ion batteries (LIBs) [8,11,12]. Electrolyte additives enhance cell performance by modifying the solid electrolyte interphase (SEI) at the graphite electrode or the passivation layer generated on the positive electrode [13–15]. Zuo et al. [16] found that the addition of MMDS to $LiCoO_2$/graphite cells modified the constituents of the passivation layer formed on the positive electrodes, which limited electrolyte oxidation. Sano et al. [17] demonstrated that there were compounds such as Li_2S and polymers like polyethylene oxide (PEO) in the SEI on the negative electrode in cells containing DTD. Electrolyte additives could therefore influence the reactivity of charged NMC materials with electrolyte at elevated temperature because they can modify the interphase between the charged electrodes and electrolytes [18]. The impact of electrolyte additives of reactivity is explored in this work.

Accelerating rate calorimetry (ARC) has been used to measure the reactivity between charged electrode materials and electrolyte at elevated temperatures, and it is able to distinguish the impact of various electrolyte additives as well [19]. In this paper, the reactivity of charged positive electrodes of SC-NMC532, NMC622A and NMC622B with electrolytes containing different electrolyte additives was methodically investigated and compared using ARC experiments. The additive systems probed were the binary electrolyte additive blends VC + DTD or VC + MMDS which have been shown to yield long lifetime cells based on SC-NMC532 and NMC622B, respectively [20]. Finally, the results from these new experiments are compared to the data collected by Ma et al. [3] on traditional NMC materials.

2. Materials and methods

2.1. Electrolyte selection

1.09 mol/kg lithium hexafluorophosphate ($LiPF_6$) (from BASF, purity 99.9%, water content 14 ppm) in ethylene carbonate (EC):ethyl methyl carbonate (EMC) (3:7 by weight, from BASF, purity 99.99%, water content < 20 ppm) was chosen to be the control electrolyte. For SC-NMC532 cells, the electrolyte being investigated contains 2% VC (from BASF, purity 99.97%) and 1% DTD (from Aldrich, purity 98%) (by weight). This electrolyte was selected based on the work of Li et al., who showed it to create SC-NMC532/graphite cells with excellent lifetime [20]. For NMC622A/graphite and NMC622B/graphite, the electrolyte being investigated contains 2% VC and 1% MMDS (from Guangzhou Tinci Co. Ltd, purity 98.70%) (by weight).

In experiments to measure the voltage to reach to the maximum capacity of three pouch cells, an electrolyte containing 2% fluoroethylene carbonate (FEC) (from BASF, purity 99.94%) by weight was used. Fig. 1 shows the molecular structures of the additives used in this study.

2.2. NMC pouch cell configuration

2.2.1. Characteristics of supplied dry cells

Dry (without electrolyte) SC-NMC532/graphite, NMC622A/graphite and NMC622B/graphite pouch cells balanced for 4.4 V operation were obtained from Li-Fun Technology (Xinma Industry Zone, Golden Dragon Road, Tianyuan District, Zhuzhou City, Hunan Province, PRC, 412000). The SC-NMC532 used in these cells was described in the paper by Li et al. [4], while NMC622A and NMC622B were provided by Umicore (Chonan, Korea). NMC622A and NMC622B have an Al_2O_3 coating and a proprietary high voltage coating, respectively. The weight ratios of NMC to conductive carbon and polyvinylidene fluoride (PVDF) binder in the electrodes were 94:4:2, 96:2:2 and 96:2:2 for SC-NMC532, NMC622A and NMC622B, respectively. During the ARC testing at elevated temperatures, the reaction rate depends on the surface area of the interphase between the electrode materials and the electrolyte [21]. Table 1 presents the BET specific surface areas of all the samples. Fig. 2 shows the scanning electron microscope (SEM) images of the surfaces of the electrodes of the different positive electrode materials.

2.2.2. Electrode filling and formation of test cells

All of the pouch cells were vacuum sealed without electrolyte in China and then delivered to Canada. Before adding electrolyte, the cells were cut open in an argon-filled glove box and transferred to the antechamber for drying at 100 °C under vacuum for 14 h to remove residual water. All the sample cells were filled with 0.85 ml electrolyte. After filling, cells were vacuum-sealed using a compact vacuum sealer (MSK-115A, MTI Corp.). Cells were then charged to 1.5 V and held at the same voltage for 24 h, to allow for wetting. Then, all the cells for ARC test were placed in a temperature box at 40 ± 0.1 °C and charged at the current corresponding to C/20 to 3.5 V. Cells were then transferred into the glove box again, cut open to release the generated gas and then vacuum sealed. Then all the cells were charged at the current corresponding to C/20 to the corresponding upper cut-off voltage (4.1 V, 4.2 V, 4.3 V or 4.4 V) and held for 1 h, and then discharged to 3.8 V. If cells generated more than 0.1 ml of gas during the second step, they were degassed and sealed once more. The gas volume was measured using Archimedes principle with cells suspended from a balance while submerged in ultrapure water. The changes in the weight of the cell suspended in ultrapure water, before and after testing are directly related to the volume changes through the change in the buoyant force.

As Fig. 3 shows, cells used to measure the voltage to reach to the maximum capacity were placed in a temperature box at 40 ± 0.1 °C and charged at the current corresponding to C/20 to 4.8 V, and then discharged to 2.8 V. All the cells were then charged to 4.9 V then discharged to 4.4 V twice. After those two cycles, the cells were charged to

Table 1
Summary of the specific surface areas of the positive electrode materials in SC-NMC532/graphite, NMC622A/graphite and NMC622B/graphite pouch cells.

Material	SC-NMC532	NMC622A	NMC622B
Specific surface area (m^2/g)	0.28	0.24	0.24

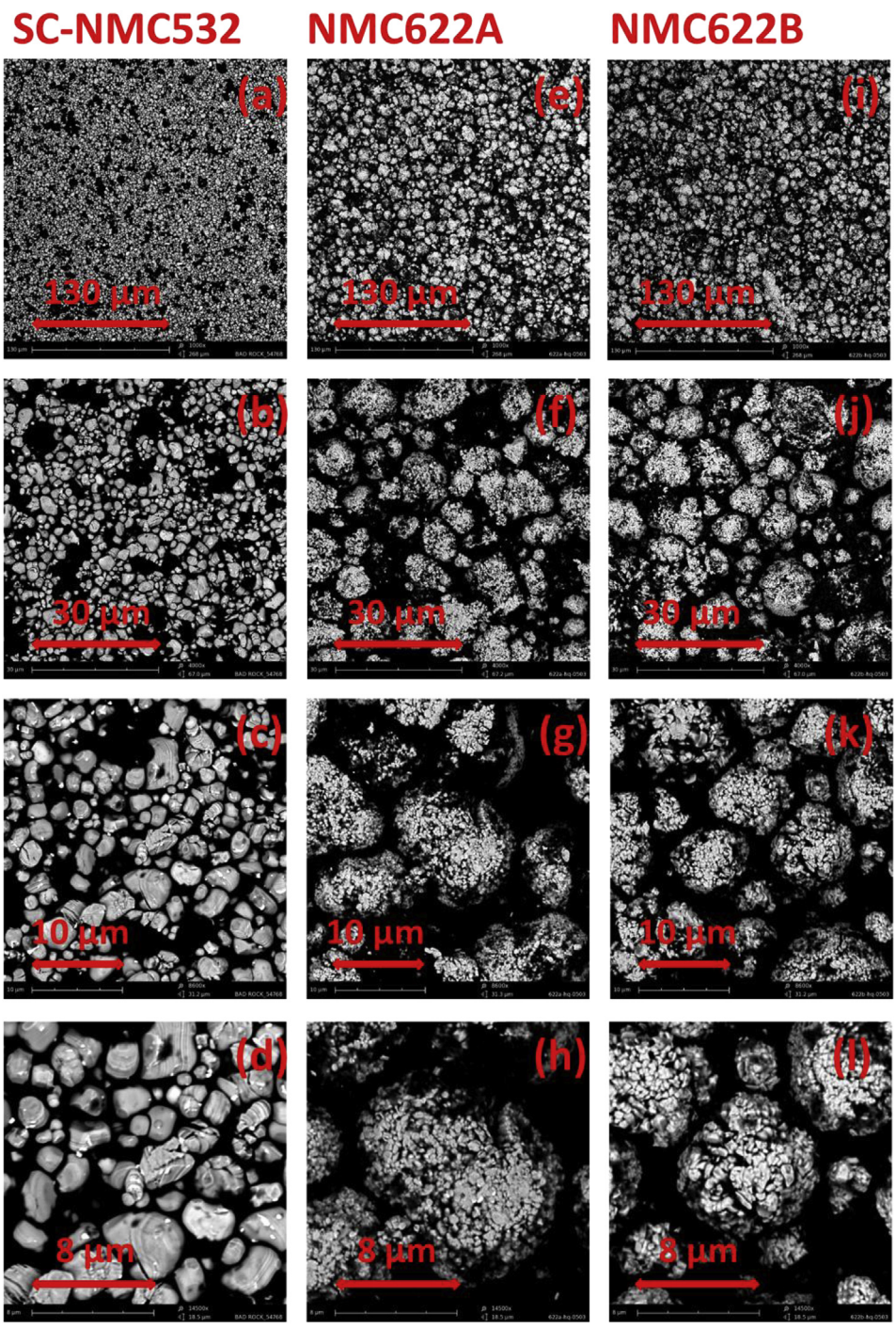

Fig. 2. SEM images of positive electrodes of (a–d) SC-NMC532, (e–h) NMC622A and (i–l) NMC622B used for ARC tests.

5.0 V then discharged to 4.4 V, and again charged to 5.0 V then discharged to 2.8 V. During this process, the cells were clamped tightly to eliminate the influence of possible generated gas. By checking the voltage and capacity versus time curves it appears the capacity to 4.9 V was the maximum capacity that the cells could attain based on de-intercalation of lithium from NMC.

2.3. Accelerating rate calorimetry (ARC) experiments

After degassing, all the cells were discharged to 3.0 V and charged to the corresponding upper cut-off potential (4.1 V, 4.2 V, 4.3 V or 4.4 V) at C/20. All the cells were then held at the upper cut-off potential for 3 h. After this step, the cells were transferred and moved into the glovebox and cut open to recover the electrodes. The electrodes were then unfolded to get the positive electrode. Then all of the positive electrodes were transferred to the antechamber for drying at room temperature under vacuum for 14 h to remove residual electrolyte. All the charged electrode powders for the ARC tests were obtained by carefully scraping from the current collectors without rinsing. Since the electrodes were adhered well to the Al foil current collectors, the scraping was quite time consuming.

In order to make the results comparable, the capacities of de-lithiated positive electrode material powder added to each sample ARC tube were kept consistent (around 15 mAh). So the mass of charged positive electrode material was adjusted for each sample. The mass of material added into each ARC tube was determined as described below:

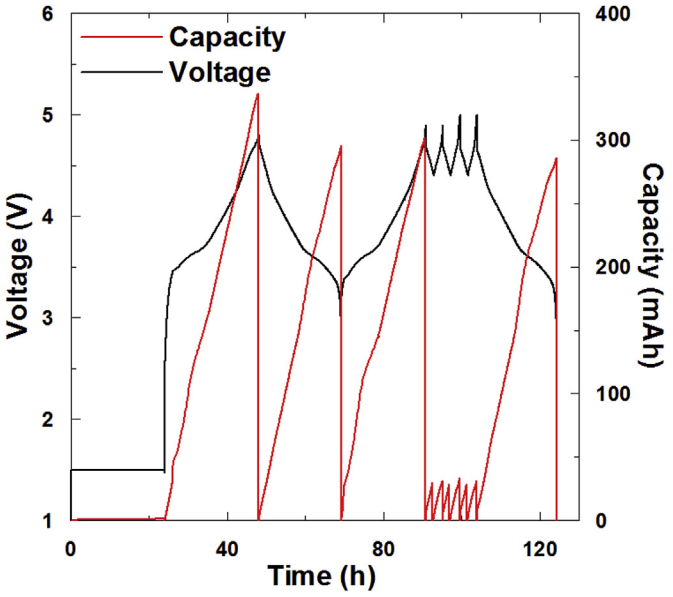

Fig. 3. Voltage and capacity versus time for pouch cells (clamped) containing selected additive 2% FEC.

The mass of positive electrode material in an SC-NMC532/graphite pouch cell was 1.27 g. When the cell was charged the first time to 4.1 V, the capacity was about 215 mAh. So the specific capacity of the SC-NMC532 material charged to 4.1 V was:

$Q_{specific}$ = 215 mAh/(1.27 g × 0.94) = 180 mAh/g

The number of moles, n, of delithiated lithium per formula unit was:

n = 180 mAh/g 3.6 C/mAh M/F = 0.65

where M = 96.7 g/mole is the formula weight of SC-NMC532 and F is Faraday's number in C/mole.

Therefore the delithiated SC-NMC532 at 4.1 V can be described as $Li_{(1-0.65)}[Ni_{0.5}Mn_{0.3}Co_{0.2}]O_2$, or $Li_{0.35}[Ni_{0.5}Mn_{0.3}Co_{0.2}]O_2$. Thus, the mass, m, of delithiated material required for the ARC test is: m = (15 mAh/180 mAh/g) (92.0/M)/0.94 = 84 mg.

In the equation above, 92.0 (g/mole) is the formula weight of $Li_{0.35}[Ni_{0.5}Mn_{0.3}Co_{0.2}]O_2$ and 0.94 is the active mass fraction of the positive electrode of SC-NMC532.

Table 2 displays the full cell capacity, specific capacity, delithiated NMC chemical formula and molar mass for the ARC test samples. In order to simulate a similar condition as in a lithium-ion cell, an appropriate amount of electrolyte was added into the ARC tube together with the charged positive electrode powder. Table 3 lists the masses of electrode material and electrolyte used for the ARC tests. The electrode:electrolyte mass ratios were kept at 3:1 for all the tests.

The ARC used in this work is an adiabatic calorimeter, so there is no heat flow between the jacket and the sample tube during the exotherm. Adiabaticity is maintained by keeping the temperature of the jacket and the sample tube the same during the exothermic regions of the measurement. The sample temperature sensor detects the temperature of the sample. There are also temperature sensors in top, side and bottom zones of the ARC. If the sample heats up due to heat released by internal reactions, a small difference in temperature between the sample and the jacket will be detected. The computer-controlled jacket will then heat up to maintain the same sample and jacket temperature. A heat-wait-search procedure was used to find the exotherms. The start temperature of ARC was set to 70 °C. Then the ARC waited for 10 min for the sample temperature to come close to the jacket temperature. The ARC waited for 15 min to detect self heating of the sample. If the sample self-heating rate (SHR) exceeded 0.03 °C/min then the exotherm was followed under adiabatic conditions as described above. The measurements were stopped automatically at 350 °C or when the SHR exceeded 20 °C/min. In order to test the reproducibility of the ARC samples, two identical ARC samples for each positive electrode were made and measured for every condition.

2.4. Inductively coupled plasma optical emission spectrometry (ICP-OES) experiments

A Perkin Elmer Optima 8000 ICP-OES Spectrometer was used for ICP-OES measurements to determine the metallic elemental composition of positive electrode materials of SC-NMC532, NMC622A and NMC622B (reported as ratios of Li, Ni, Mn and Co). A 0 ppm "blank" was used, as well as two standard solutions of 0.5 ppm Li and 1 ppm Ni, Mn, Co, another containing 1 ppm Li and 2 ppm Ni, Mn and Co. Standards were prepared by accurately pipetting 1000 ppm single-element standards (Sigma-Aldrich) and diluting the standards in 2% HNO_3. The 2% HNO_3 used for sample preparation was prepared using deionized water (18.2 MΩ-cm). In order to stay approximately in the 0.5–2 ppm region, around 10 mg of the NMC sample powder was dissolved in 2 mL aqua regia (1:3 HNO_3:HCl) and left overnight to dissolve fully before dilution in 2% HNO_3. 10 µL was then pipetted and diluted with about 12 mL of 2% HNO_3. Table 4 shows a summary of the Li contents determined from the cell capacities and from the ICP-OES results.

Table 2
The chemical composition of the delithiated NMC grades, the molar mass, the full cell capacity and the specific capacity of the different positive electrodes charged to the different upper cut-off potentials.

Positive material	Voltage (V)	Chemical formula of the delithiated NMC	Formula weight (g/mol)	Capacity of full cell (mAh)	Specific capacity (mAh/g)
SC-NMC532 (96.66 g/mol)	4.1	$Li_{0.35}[N_{0.5}M_{0.3}C_{0.2}]O_2$	92.04	215	180
	4.2	$Li_{0.32}[N_{0.5}M_{0.3}C_{0.2}]O_2$	91.85	224	188
	4.3	$Li_{0.28}[N_{0.5}M_{0.3}C_{0.2}]O_2$	91.56	238	199
	4.4	$Li_{0.23}[N_{0.5}M_{0.3}C_{0.2}]O_2$	91.18	256	214
	4.9	$Li_{0.11}[N_{0.5}M_{0.3}C_{0.2}]O_2$	90.36	295	247
NMC622A (96.93 g/mol)	4.1	$Li_{0.37}[N_{0.6}M_{0.2}C_{0.2}]O_2$	92.55	221	174
	4.2	$Li_{0.31}[N_{0.6}M_{0.2}C_{0.2}]O_2$	92.14	242	191
	4.3	$Li_{0.27}[N_{0.6}M_{0.2}C_{0.2}]O_2$	91.84	257	203
	4.4	$Li_{0.22}[N_{0.6}M_{0.2}C_{0.2}]O_2$	91.52	273	215
	4.9	$Li_{0.14}[N_{0.6}M_{0.2}C_{0.2}]O_2$	90.99	300	237
NMC622B (96.93 g/mol)	4.1	$Li_{0.37}[N_{0.6}M_{0.2}C_{0.2}]O_2$	92.57	222	174
	4.2	$Li_{0.32}[N_{0.6}M_{0.2}C_{0.2}]O_2$	92.21	240	188
	4.3	$Li_{0.27}[N_{0.6}M_{0.2}C_{0.2}]O_2$	91.88	257	201
	4.4	$Li_{0.23}[N_{0.6}M_{0.2}C_{0.2}]O_2$	91.58	272	213
	4.9	$Li_{0.13}[N_{0.6}M_{0.2}C_{0.2}]O_2$	90.91	306	240

Table 3
Summary of the electrode mass and electrolyte mass used for each ARC test sample.

	4.1 V		4.2 V		4.3 V		4.4 V	
	Electrode (mg)	Electrolyte (mg)	Electrode (mg)	Electrolyte (mg)	Electrode (mg)	Electrolyte (mg)	Electrode (mg)	Electrolyte (mg)
SC-NMC532	84	28	81	27	76	25	70	23
NMC622A	86	28	78	26	73	24	68	23
NMC622B	86	29	79	26	74	24	69	23

Table 4
Summary of the Li contents of the samples from cell capacities and from ICP-OES results.

Pouch cells	Voltage (V)	Mass of positive materials (mg)	n (delithiated lithium)	Li (from cell capacity)	Li (ICP-OES)	difference
SC-NMC532	4.1	1.27	0.65	0.35	0.31	0.04
	4.2		0.68	0.32	0.25	0.08
	4.3		0.72	0.28	0.20	0.08
	4.4		0.77	0.23	0.09	0.13
	4.9		0.89	0.11	/	/
NMC622A	4.1	1.32	0.63	0.37	0.31	0.06
	4.2		0.69	0.31	0.21	0.10
	4.3		0.73	0.27	0.14	0.12
	4.4		0.78	0.22	0.04	0.18
	4.9		0.86	0.14	/	/
NMC622B	4.1	1.33	0.63	0.37	0.37	0.00
	4.2		0.68	0.32	0.29	0.03
	4.3		0.73	0.27	0.24	0.03
	4.4		0.77	0.23	0.19	0.04
	4.9		0.87	0.13	/	/

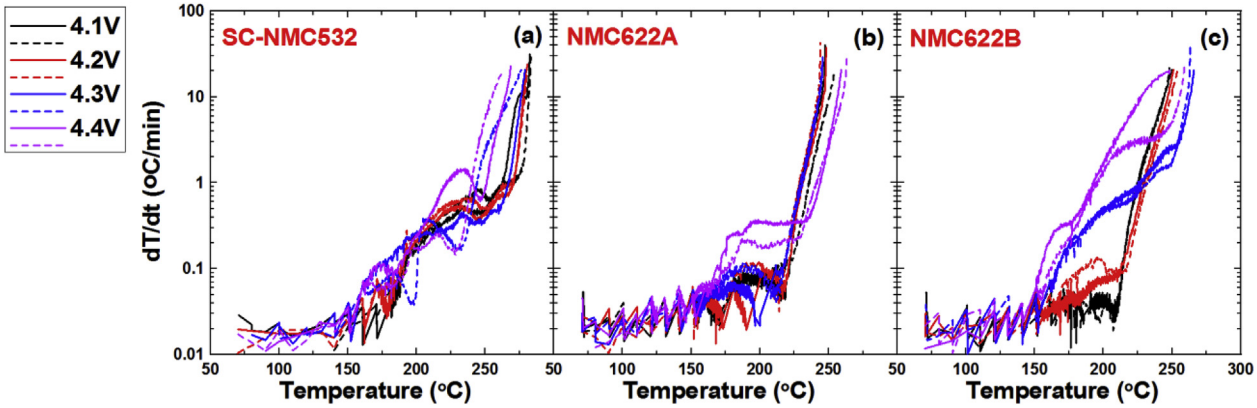

Fig. 4. SHR vs. temperature for delithiated (a) SC-NMC532, (b) NMC622A and (c) NMC622B reacting with control electrolyte 1.09 mol/kg $LiPF_6$ in EC: EMC (3:7) at different cut-off voltages. The results for duplicate samples are given as a dashed line in each panel.

The ICP-OES results for the NMC622A cells showed that when the cells were charged to 4.4 V, there was little Li left in the positive electrodes. On the contrary, the experiments measuring maximum capacity (Fig. 3) indicated that when cells were charged from 4.4 V to 4.9 V that more lithium (about $\Delta n = 0.1$) could be extracted than suggested by the ICP-OES results. Furthermore, the NMC622A and NMC622B materials differ only by the thin coating (less than 1% by weight) applied. The materials should have the same value of n at the same potential. Table 4 shows that this is the case for the lithium contents determined from the cell capacity but not for the lithium contents determined from ICP-OES. The electrochemical and ICP-OES results agree well for NMC622B but not for NMC622A. Therefore, the Li content calculated from cell capacity was deemed to be more accurate than the results from ICP-OES and will be used in the analysis below.

3. Results and discussion

Fig. 4 shows the SHR versus temperature results for delithiated SC-NMC532, NMC622A and NMC622B harvested at various cut-off voltages reacting with 1.09 mol/kg $LiPF_6$ in EC: EMC (3:7). Each experiment was repeated and the results were highly reproducible. The results for duplicate samples are given as dashed lines in each panel. The maximum SHR of all the test samples eventually exceeded 20 °C/min. Fig. 4a shows that the onset temperature for a sustained exotherm in SC-NMC532 charged to 4.1, 4.2 or 4.3 V was about 150 °C for all three samples. The SHR of SC-NMC532 charged to 4.4 V increased dramatically at around 150 °C. Fig. 4b indicates that the SHR of NMC622A charged to 4.2 V or 4.3 V is slightly higher than that of NMC622A charged to 4.1 V between approximately 150 °C and 190 °C. Then the SHR of NMC622A charged to 4.1, 4.2 or 4.3 V increased significantly at around 215 °C. Like SC-NMC532, the SHR of NMC622A charged to 4.4 V increased markedly much earlier (~175 °C). Fig. 4c illustrates that the onset temperature for a sustained exotherm in NMC622B charged to 4.1 or 4.2 V is about 150 °C for two samples. NMC622B charged to 4.4 V has an earlier onset temperature (around 140 °C) and the highest SHR during the exotherm compared to the other cut-off voltages.

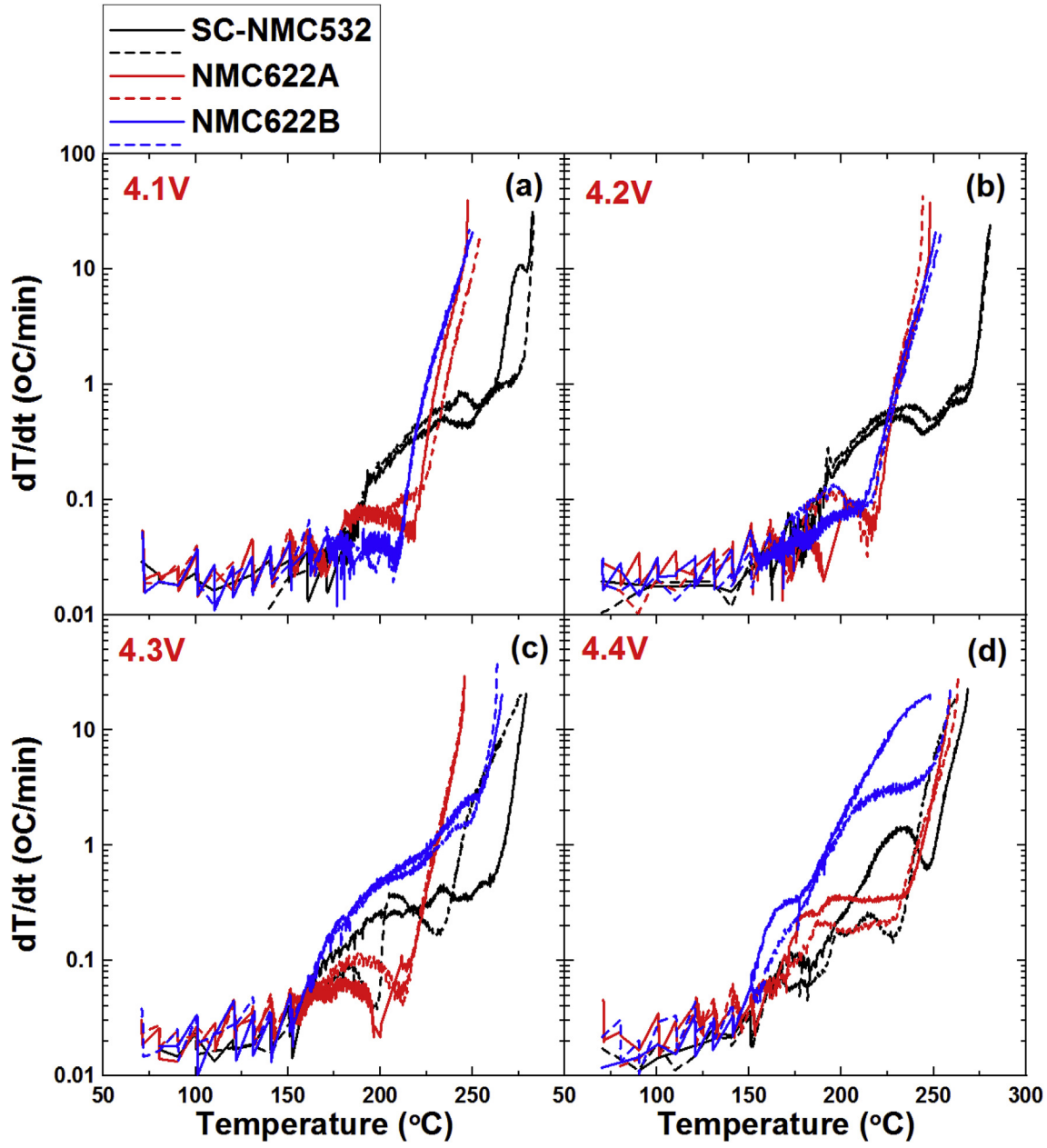

Fig. 5. SHR vs. temperature for different delithiated positive electrodes reacting with control electrolyte 1.09 mol/kg $LiPF_6$ in EC: EMC (3:7) at (a) 4.1 V, (b) 4.2 V, (c) 4.3 V and (d) 4.4 V. The results for duplicate samples are given as a dashed line in each panel.

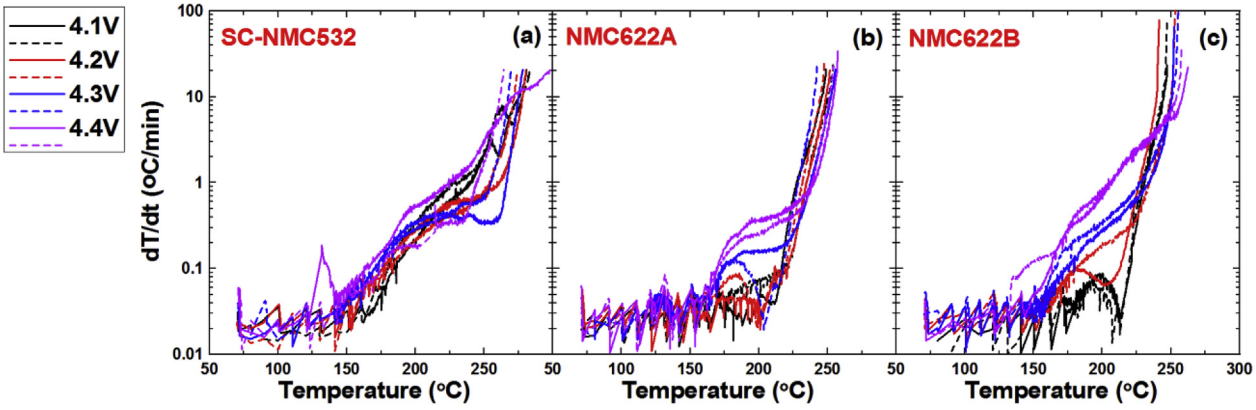

Fig. 6. SHR vs. temperature for delithiated (a) R532, (b) 622A and (c) 622B reacting with electrolyte 1.09 mol/kg $LiPF_6$ in EC: EMC (3:7) containing additives (2% VC + 1% DTD for SC-NMC532, 2% VC + 1% MMDS for NMC622A and NMC622B) at different cut-off voltages. The results for duplicate samples are given as a dashed line in each panel.

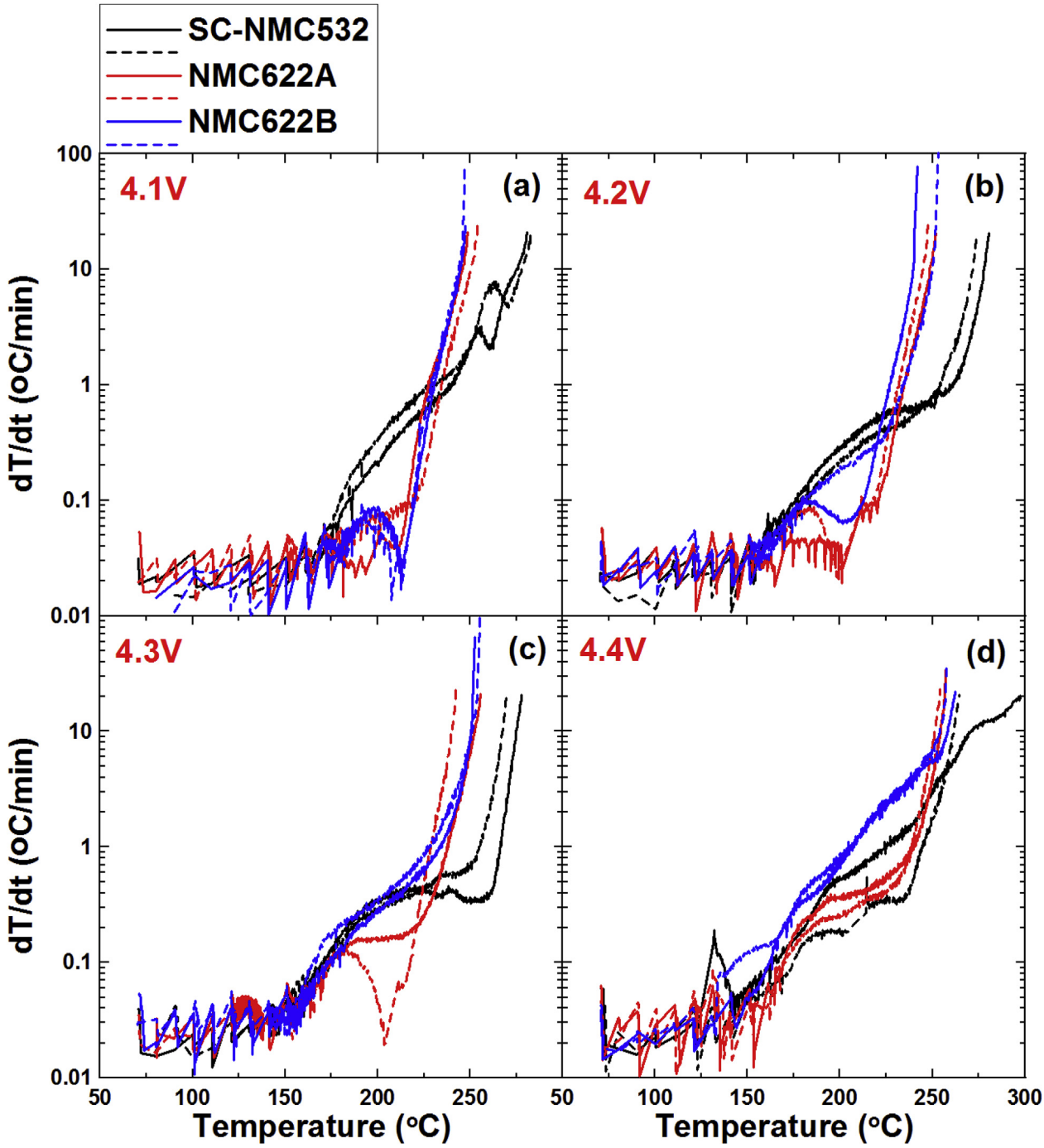

Fig. 7. SHR vs. temperature for the different delithiated positive electrodes reacting with electrolyte 1.09 mol/kg $LiPF_6$ in EC: EMC (3:7) containing additives (2% VC + 1% DTD for SC-NMC532, 2% VC + 1% MMDS for NMC622A and NMC622B) at (a) 4.1 V, (b) 4.2 V, (c) 4.3 V and (d) 4.4 V. The results for duplicate samples are given as a dashed line in each panel.

Fig. 5 shows the SHR versus temperature results for the different delithiated positive electrodes of SC-NMC532, NMC622A and NMC622B reacting with 1.09 mol/kg $LiPF_6$ in EC: EMC (3:7) at (a) 4.1 V, (b) 4.2 V, (c) 4.3 V and (d) 4.4 V. Fig. 5a–b shows that NMC622A and NMC622B demonstrate similar exothermic behavior over the entire temperature range at 4.1 V and 4.2 V, respectively, and they are substantially more reactive than SC-NMC532 at the same potential. NMC622B is noticeably more reactive than the other samples at 4.3 V and 4.4 V.

Fig. 6 explores the impact of electrolyte additives (2% VC + 1% DTD for SC-NMC532, 2% VC + 1% MMDS for NMC622A and NMC622B) on the reactivity of the charged electrode materials with electrolyte. Fig. 6a demonstrates there is no obvious heat release until approximately 150 °C for SC-NMC532 charged to 4.1 V reacting with electrolyte containing 2% VC + 1% DTD, after which the SHR increased rapidly. Increasing the upper cut-off potential generally intensified the reaction between charged SC-NMC532 and electrolyte with additives 2% VC and 1% DTD at elevated temperatures. Fig. 6b shows that the onset temperatures for a sustained exotherm in NMC622A charged to 4.1, 4.2, 4.3 and 4.4 V with electrolyte containing the additives 2% VC and 1% MMDS are approximately 220 °C, 200 °C, 175 °C, and 165 °C, respectively. The higher the cut-off voltage, the

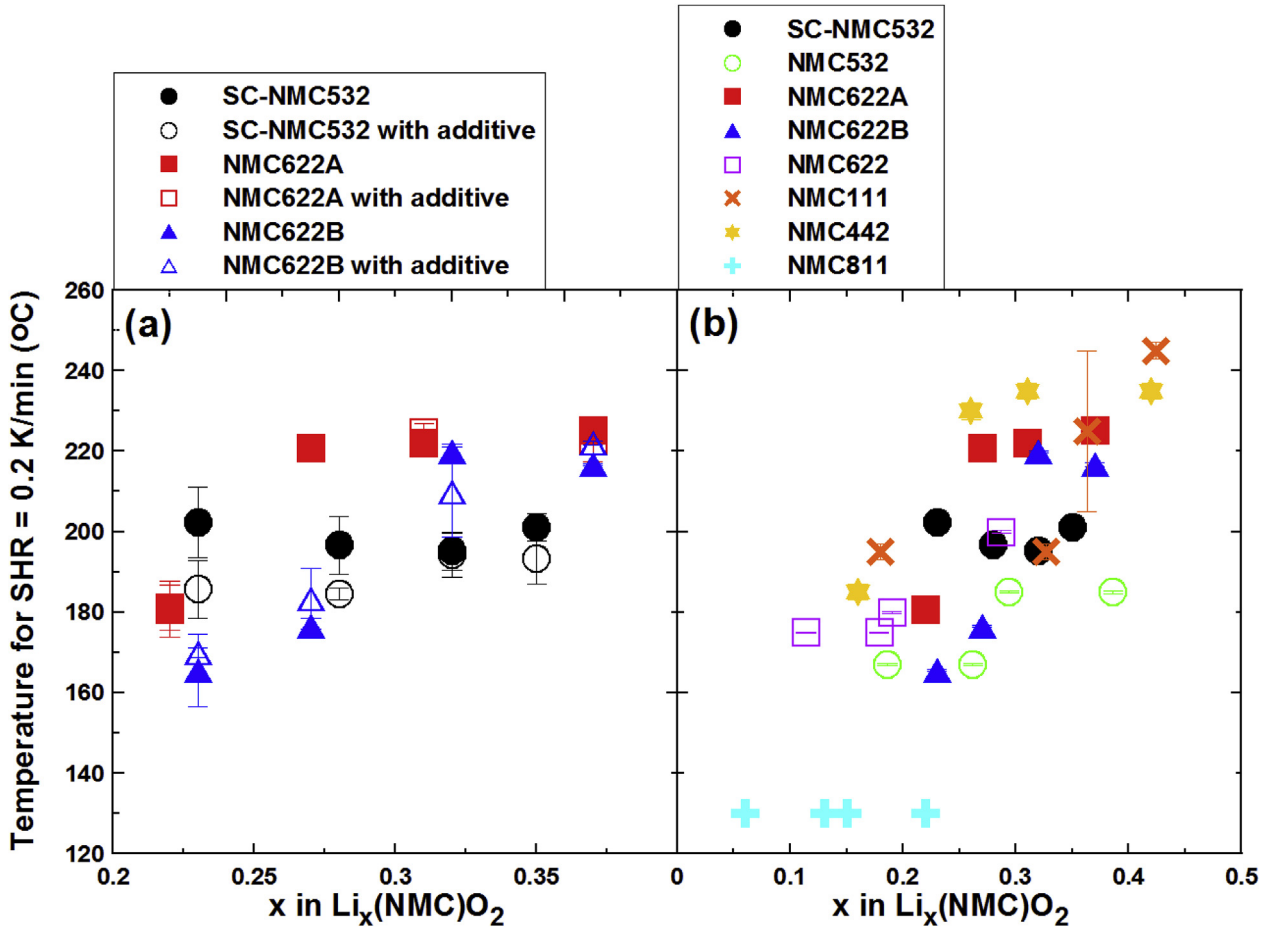

Fig. 8. The temperature where the self-heating rate reaches 0.2 °C/min plotted versus the remaining lithium content, x, in $Li_x[NMC]O_2$. This compares all the materials at the same degree of delithiation. Results from Ma et al. [3] are included in Fig. 7b.

lower the onset temperature. Fig. 6c shows that the onset temperature for a sustained exotherm in NMC622B with electrolyte containing the additives VC and MMDS charged to 4.1 V is approximately 210 °C. For 4.2, 4.3 and 4.4 V, the onset temperatures are 180 °C, 160 °C and 150 °C, respectively. When the cut-off voltages increased, the NMC622B electrodes had lower onset temperatures.

Fig. 7 shows SHR versus temperature results for the different delithiated pouch cells reacting with electrolyte containing additives (2% VC + 1% DTD for SC-NMC532, 2% VC + 1% MMDS for NMC622A and NMC622B) at (a) 4.1 V, (b) 4.2 V, (c) 4.3 V and (d) 4.4 V. Fig. 7a and b shows that NMC622A and NMC622B demonstrated similar exothermic behavior to each other over the entire temperature range at 4.1 V and 4.2 V, respectively, and they are more reactive than SC-NMC532 at the same potential at temperatures above approximately 250 °C. NMC622B is more reactive than the other samples at 4.3 V and 4.4 V.

Even though Figs. 4–7 compared the various samples at the same potential, they are not at the same specific capacity or the same degree of Li delithiation. In order to make this comparison clearly, the point where the SHR first reached 0.2 °C/min was plotted versus the Li content, x, in $Li_x[NMC]O_2$, for each sample (extracted from Table 2 where the Li content was calculated from the cell capacity). Wang et al. [22] argued that a SHR of 0.2 °C/min (in these ARC samples) signifies the temperature where positive electrode-electrolyte reactions will cause thermal runaway in 18650-size cells. Fig. 8 illustrates the temperature where the SHR first reaches 0.2 °C/min plotted versus Li content. Two results were measured for each data point and the error bar represents the standard deviation between the data.

Fig. 8a suggests that NMC622A showed an excellent safety performance when Li content is above 0.25. While with a cut-off voltage of 4.4 V, SC-NMC532 is more stable and controlled. Since Mn^{4+} can stabilize the oxide matrix even in a highly delithiated state and it is not electrochemically active, the amount of Mn might control the thermal reactivity of NMC materials with electrolyte [2,23]. The higher the Ni content in delithiated NMC, the lower the onset temperature of the phase transitions to spinel and rocksalt phases and the larger the amount of released oxygen [24]. The generated oxygen will accelerate the combustion of the solvent and produce more heat. Thus, higher Ni content and lower Mn and Co contents normally lead to lower onset temperatures and higher SHR for exothermic reactions. On the basis of this analysis, SC-NMC532 is generally relatively safer than NMC622A and NMC622B at 4.4 V. Comparing the testing with and without additives (2% VC + 1% DTD for SC-NMC532, 2% VC + 1% MMDS for NMC622A and NMC622B), the results show that generally these additives do not strongly affect the reactivity of the charged positive electrode materials.

Fig. 8b includes the results from Ma et al. [3] which investigated uncoated NMC111, NMC442, NMC532, NMC 622 and NMC811 using the same methods as reported here. Those samples had similar BET surface areas to the materials studied here [3]. Fig. 8b suggests that NMC442 shows excellent safety performance when x is about 0.25. That is NMC442, at 4.5 V shows less reactivity with electrolyte than SC-NMC532, NMC622A and NMC622B at 4.3 V, NMC111 and NMC532 at 4.4 V and NMC811 at 4.2 V. The most striking feature of Fig. 8b is the intense reactivity of charged NMC811 with electrolyte compared to all the other NMC grades. This suggests there will need to be clever approaches used to make cells using NMC811 safe for consumer applications. Fig. 8b also shows that the single crystal NMC532 sample studied here shows better thermal stability than traditional NMC532.

4. Conclusions

The reactivity between charged SC-NMC532, NMC622A and NMC622B positive electrode materials and control electrolyte 1.09 mol/kg $LiPF_6$ in EC: EMC (3:7) with or without additives (2% VC + 1% DTD for SC-NMC532, 2% VC + 1% MMDS for NMC622A and NMC622B) at elevated temperatures has been systematically studied using ARC. The results indicate that the reactivity of the positive electrode materials with electrolyte was influenced by the upper cutoff voltages. As the upper cutoff potential rose, the onset temperature decreased, and the SHR went up, especially at 4.4 V, reflecting a trade-off between safety and high energy density. The single crystal NMC532 had less reactivity with electrolyte than a traditional polycrystalline NMC532 studied by Ma et al. using the same methods. The use of the electrolyte additives tested here did not strongly impact the reactivity of the charged materials.

Comparison of the results measured here for the coated samples of NMC622A and NMC622B to the uncoated NMC622 (Fig. 8b) presented by Ma et al. [3] suggests that the coatings do little to enhance the thermal stability of traditional polycrystalline NMC622. Additionally, by comparing the results from Ma et al. [3], it is clear that charged NMC811 is significantly more reactive with electrolyte than the other NMC grades.

Acknowledgements

This research was supported by NSERC and Tesla Motors. Q.H acknowledges the support of the China Scholarship Council. L.M. acknowledges the support of the Killam Trusts. The authors thank Dr. Jing Li (formerly of BASF) for providing some of the solvents and salts used in this work.

References

[1] K.J. Nelson, G.L. d'Eon, A.T.B. Wright, L. Ma, J. Xia, J.R. Dahn, J. Electrochem. Soc. 162 (2015) A1046–A1054.
[2] H. Kim, S.-M. Oh, B. Scrosati, Y.-K. Sun, Adv. Battery Technol. Electr. Veh. (2015) 191–241.
[3] L. Ma, M. Nie, J. Xia, J.R. Dahn, J. Power Sources 327 (2016) 145–150.
[4] J. Li, A.R. Cameron, H. Li, S. Glazier, D. Xiong, M. Chatzidakis, J. Allen, G.A. Botton, J.R. Dahn, J. Electrochem. Soc. 164 (2017) A1534–A1544.
[5] J. Kim, H. Lee, H. Cha, M. Yoon, M. Park, J. Cho, Adv. Energy Mater. (2017), http://dx.doi.org/10.1002/aenm.201702028.
[6] M. Broussely, P. Biensan, F. Bonhomme, P. Blanchard, S. Herreyre, K. Nechev, R.J. Staniewicz, in: 2005: pp. 90–96.
[7] J.C. Burns, A. Kassam, N.N. Sinha, L.E. Downie, L. Solnickova, B.M. Way, J.R. Dahn, J. Electrochem. Soc. 160 (2013) A1451–A1456.
[8] J.C. Burns, R. Petibon, K.J. Nelson, N.N. Sinha, A. Kassam, B.M. Way, J.R. Dahn, J. Electrochem. Soc. 160 (2013) A1668–A1674.
[9] J.C. Burns, G. Jain, A.J. Smith, K.W. Eberman, E. Scott, J.P. Gardner, J.R. Dahn, J. Electrochem. Soc. 158 (2011) A255.
[10] L. Ma, J. Xia, J.R. Dahn, J. Electrochem. Soc. 162 (2015) A1170–A1174.
[11] J. Xia, N.N. Sinha, L.P. Chen, J.R. Dahn, J. Electrochem. Soc. 161 (2013) A264–A274.
[12] J. Xia, N.N. Sinha, L.P. Chen, G.Y. Kim, D.J. Xiong, J.R. Dahn, J. Electrochem. Soc. 161 (2013) A84–A88.
[13] S.S. Zhang, J. Power Sources 162 (2006) 1379–1394.
[14] K. Xu, Chem. Rev. 104 (2004) 4303–4417.
[15] M. Nie, D. Chalasani, D.P. Abraham, Y. Chen, A. Bose, B.L. Lucht, J. Phys. Chem. C 117 (2013) 1257–1267.
[16] X. Zuo, C. Fan, X. Xiao, J. Liu, J. Nan, J. Power Sources 219 (2012) 94–99.
[17] A. Sano, M. Kurihara, K. Ogawa, T. Iijima, S. Maruyama, J. Power Sources 192 (2009) 703–707.
[18] E.P. Roth, C.J. Orendorff, Interface 21 (2012) 45–50.
[19] L. Ma, J. Xia, X. Xia, J.R. Dahn, J. Electrochem. Soc. 161 (2014) A1495–A1498.
[20] J.R.D. Jing Li, Hongyang Li, Will Stone, Stephen Glazier, (n.d.) (to be submitted to J. Electrochem. Soc.).
[21] D.D. MacNeil, J. Electrochem. Soc. 146 (1999) 3596.
[22] Y. Wang, J. Jiang, J.R. Dahn, Electrochem. Commun. 9 (2007) 2534–2540.
[23] K.-S. Lee, S.-T. Myung, K. Amine, H. Yashiro, Y.-K. Sun, J. Electrochem. Soc. 154 (2007) A971.
[24] S.M. Bak, E. Hu, Y. Zhou, X. Yu, S.D. Senanayake, S.J. Cho, K.B. Kim, K.Y. Chung, X.Q. Yang, K.W. Nam, ACS Appl. Mater. Interfaces 6 (2014) 22594–22601.